

A FEM Model for Wave-Induced Pore Pressure Response around a Pile Foundation

Xiaojun Li¹, Bing Yang¹, Fuping Gao¹, Jun Zang²

¹ Key laboratory for Hydrodynamics and Ocean Engineering, Institute of Mechanics, Chinese Academy of Sciences, Beijing, China

² Department of Architecture & Civil Engineering, University of Bath, Bath, UK

ABSTRACT

A three-dimensional FEM model is proposed and verified with existing experimental data for simulating wave-induced transient and residual pore pressure responses in the soil around pile foundations. The numerical results show that the residual pore pressure tends to be amplified around the pile foundation, especially at the bottom of pile foundation. Parametric study indicates that the residual pore pressure in the vicinity of the pile foundation increases and the amplitude of transient pore pressure decreases with the decrease of soil permeability. The effect of pile diameter on the oscillatory pore pressure is much more obvious than that on the build-up of residual pore pressure.

KEY WORDS: ocean wave; pile foundation; seabed; transient and residual pore pressure; FEM

INTRODUCTION

Pile foundations have been widely used in coastal and ocean engineering, such as oil platforms, long-spanning bridges and offshore wind farm, etc. Under the action of ocean waves, pore water pressure may be induced in the seabed around pile foundations, which is usually accompanied by the reduction of effective stresses. In some severe conditions, i.e. hurricanes or storms, the soil around pile foundations may be liquefied, resulting in large displacements of the pile foundation and eventual collapse of upper structures. Thus, a proper evaluation of wave-induced pore pressure around pile foundations is crucial for the geotechnical design of maritime structures.

Generally, there are two significant mechanisms accounting for wave-induced pore pressure responses, which are also observed in laboratory experiments and field measurements (Nago *et al.*, 1993). The first mechanism, termed as transient or oscillatory pore pressure, is characterized by the attenuation of amplitude and the phase lag within the seabed. The other is residual or build-up of pore pressure caused by the compress of soil skeleton leading to the generation of excess pore pressure. The latter is much similar to the pore pressure responses induced by earthquakes.

Since 1970s, wave-induced pore pressure responses and liquefaction within porous seabed have gradually been concerned by marine geotechnical engineers and researchers. Based on the conventional Biot consolidation equations (Biot, 1941), the transient characteristics of

excess pore pressure for infinite seabed has been studied theoretically by Yamamoto *et al.* (1978). Then, under the same framework, a series of analytical solutions have been accomplished by considering the finite thickness of seabed and orthotropic nature of soil (Jeng and Hsu, 1996; Jeng, 1997). On the other hand, the residual or build-up of pore pressure has been investigated by some researchers (Seed and Rahman, 1978; McDougal *et al.*, 1989; Sumer and Fredsøe, 2002). The empirical relationships obtained from dynamic triaxial or simple shear tests have been employed to model the pore pressure generation under undrained condition (DeAlba *et al.*, 1975; Seed *et al.*, 1976). The aforementioned research, however, mainly focused on one of the mechanisms for the pore pressure responses individually. In fact, the wave-induced transient and residual pore pressure responses are coupled.

Numerous studies have also been conducted to investigate the pore pressure responses or liquefaction around marine structures. For instance, Rahman *et al.* (1977) developed a practical procedure to analyze the pore pressure response and soil liquefaction under Ekofisk oil tank. Based on flume experiments, Sumer *et al.* (1999, 2006) have systematically examined the pore pressure response around the pipeline buried in the soil and sinking/floating of pipelines. A review on pore pressure responses of soil around offshore structures could also be found in Jeng (2003). However, the pore pressure response in the soil around pile foundations has not been well understood.

In this study, a FEM model is proposed to simultaneously simulate the wave-induced transient and residual pore pressure responses in the soil around pile foundations. The numerical model is verified with the existing experimental data from Sumer *et al.* (1999). The pore pressure responses in the vicinity of pile foundation have been compared with those in the absence of pile foundation. Parametric study is also employed to examine the influences of soil permeability and pile diameter on transient and residual pore pressure responses near the pile foundation.

NUMERICAL MODEL

The wave-induced pore pressure response around pile foundations is investigated in the present study, which involves the interaction between wave, soil and pile, as shown in Fig. 1. The profile of the pile foundation is characterized by the diameter D and the depth of embedment l . The wave is assumed to propagate in the positive x -direction, while the z -direction is upward from the interface between water and porous seabed.

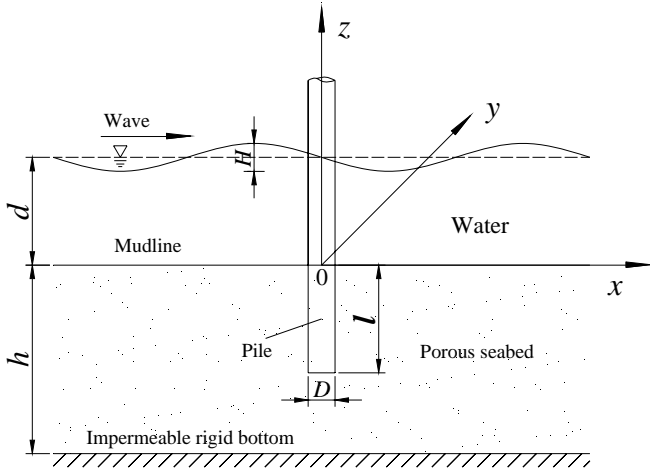


Fig.1 Definition of wave-seabed-pile interaction problem.

Governing equations

According to the Darcy's law and the continuity of pore water, the governing equation for the flow of pore water within seabed can be deduced with the assumptions of compressible pore water and soil skeleton:

$$\frac{k_s}{\gamma_w} \left(\frac{\partial^2 p}{\partial x^2} + \frac{\partial^2 p}{\partial y^2} + \frac{\partial^2 p}{\partial z^2} \right) - \frac{n}{K'} \frac{\partial p}{\partial t} = \frac{\partial \varepsilon}{\partial t} \quad (1)$$

where p is the excess pore pressure, k_s is the coefficient of soil permeability, γ_w is the unit weight of pore fluid, and n is the porosity of soil. It is noted that K' is the apparent bulk modulus of pore water, which is defined by

$$\frac{1}{K'} = \frac{1}{K} + \frac{1 - S_r}{P_{w0}} \quad (2)$$

in which K is the true bulk modulus of elasticity of water (taken as $2 \times 10^9 \text{ N/m}^2$), S_r is the degree of saturation and $P_{w0} = \gamma_w d$ is the absolute pressure (d is the water depth).

It is also noted that ε is the volumetric strain of soil skeleton and the volume reduction is considered positive. According to the analysis by Seed and Rahman (1978) on the soil liquefaction under cyclic loading, there exist relationship between volume change and the change of effective bulk stress, which corresponds to the dissipation of pore pressure from the soil skeleton for fully drained condition, that is

$$\frac{\partial \varepsilon}{\partial t} = m_v \left(\frac{\partial p}{\partial t} - \psi \right) \quad (3)$$

where ψ is regarded as source term, and defined by the rate of pore pressure generation for undrained soil, i.e. $\psi = \frac{\partial u_g}{\partial t}$ (u_g is the amount

of pore pressure generation). For the linear elastic material under three-dimensional condition, the coefficient of volume compressibility can be written as

$$m_v = \frac{1 - 2\mu}{6G(1 + \mu)} \quad (4)$$

Substituting (3) into (1), we have

$$\frac{\partial p}{\partial t} = \frac{1}{n/K' + m_v} \left(\frac{k_s}{\gamma_w} \nabla^2 p + m_v \psi \right) \quad (5)$$

To solve the above equation, it is necessary to describe the amount of pore pressure generation u_g in undrained soil. Here, it is determined by (Seed *et al.*, 1976)

$$\frac{u_g}{\sigma_0} = \frac{2}{\pi} \arcsin(N/N_i)^{1/2\theta} \quad (6)$$

in which $\sigma_0 = \frac{(1 + 2K_0)}{3} \gamma' z$ is the initial effective normal stress, where

K_0 is the coefficient of lateral earth pressure and γ' is the submerged specific weight of soil. θ is the empirical constant, and a typical value of 0.7 is set by Seed *et al.* (1976). N_i is the number of shear stress cycles required to cause the initial liquefaction, which is usually related to the cyclic shear stress ratio τ/σ_0' .

$$N_i = \left(\frac{1}{\alpha} \frac{\tau}{\sigma_0'} \right)^{1/\beta} \quad (7)$$

where α and β are empirical constants, determined by the soil type and relative density of soil (McDough *et al.*, 1989). τ represents the amplitude of cyclic shear stress. In this study, the analytical solution by Jeng and Hsu (1996) has been employed to be as the initial value of numerical modeling. The amplitude of cyclic shear stress can be written as

$$\tau = p_0 [(C_1 - C_2 kz) e^{-kz} - (C_3 - C_4 kz) e^{kz} + k\delta (C_5 e^{-\delta z} - C_6 e^{\delta z})] \quad (8)$$

Based on the linear wave theory, $p_0 = \gamma_w H / 2 \cosh(kd)$ is the amplitude of pressure at the surface of seabed, where H is wave height, k is wave number, and d is water depth. C_i ($i=1, \dots, 6$) and δ are parameters closely related to the wave characteristics and soil properties. The details can be found in the paper by Jeng and Hsu (1996). The equation (8) has shown that the amplitude of shear stress τ in finite thickness of seabed is determined by both wave and soil characteristics.

Initial and boundary conditions

In order to solve the aforementioned governing equation (5), the initial and boundary conditions are set as follows: (i) at the surface of seabed ($z=0$), the pore pressure is equal to the surface pressure induced by the linear progressive waves, that is $p = p_0 \cos(kx - \omega t)$, where ω is wave frequency; (ii) at the bottom of seabed ($z = -h$) and the interface between soil and pile foundation ($x^2 + y^2 = D^2/4$ or $z=-l$), no flow occurs. i.e. $\frac{\partial p}{\partial n} = 0$; (iii) a wave length of L in x -direction is chosen to

apply to the periodic-type lateral boundary, which obeys the principle of repeatability (Zienkiewicz and Scott, 1972), that is, $p|_{x=-L/2} = p|_{x=L/2}$; (iv) according to the symmetric characteristics of linear waves and geometric profile of pile foundation, the proposed numerical model can be simplified as a 3-D symmetric problem in x - z plane (see Fig.2), thus Newman boundary condition $\mathbf{n} \cdot \nabla p = 0$ is used to simulate the symmetric boundary condition at $y=0$.

Fig.2 shows the computation domain of the numerical model and the finite element mesh used in the present study. Quadratic Lagrange elements are adopted and finer meshes are divided in the vicinity of pile foundation to ensure the accuracy of numerical modeling. Numerical tests demonstrated that a time step of $T/10$ is necessary to simulate both components of transient and residual pore pressure properly. Meanwhile, the pore pressure distribution is approximately the same around the pile for the width of calculation zone (in the y -direction)

from $1.8D$ up to $2.5D$, indicating the width of $2.0D$ is sufficient to eliminate the boundary effect. D is the pile diameter, h is the thickness of seabed (see Fig. 2).

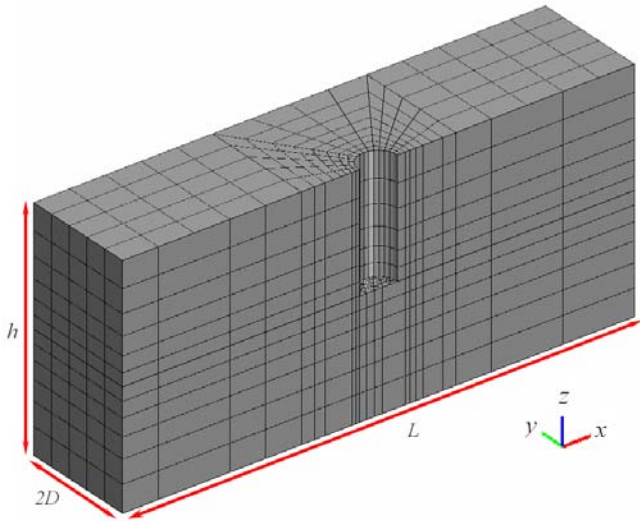
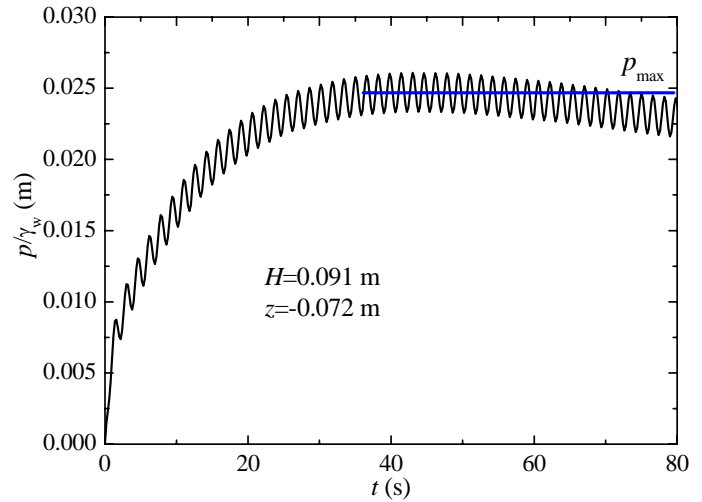


Fig.2 Sketch of 3-D numerical model and FE mesh.

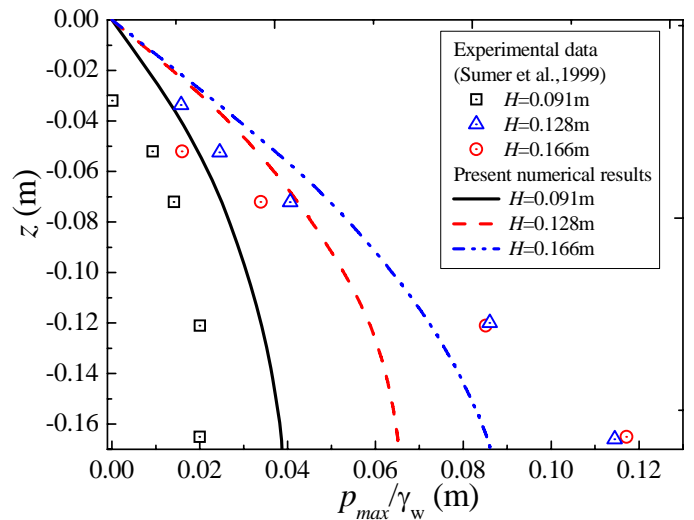
RESULTS AND DISCUSSIONS

Verification of numerical model

To verify the numerical model, the experimental data from Sumer *et al.* (1999) for undisturbed-flow case are employed. For comparison, wave and soil parameters used in the numerical model are consistent with those in the experiments by Sumer *et al.* (1999), as shown in the caption of Fig.3. Fig.3 (a) illustrates the time development of pore pressure at $z=-0.072\text{m}$. It can be seen from the figure that the two mechanisms, i.e. transient and residual pore pressures, exist simultaneously. The residual pore pressure gradually increases at the initial stage (e.g. $t < 35\text{s}$) and reaches the maximum value at certain time (e.g. $t = 35\text{s}$ in the figure). It then tends to decrease slightly at the last stage. This pattern is in accordance with the physical observations by Sumer *et al.* (1999). Comparisons of vertical distributions of the maximum value (p_{\max}) of residual pore pressure within the soil between the present numerical results and the experimental data (Sumer *et al.*, 1999) are shown in Fig.3 (b). It is indicated that the tendency for the numerical results, i.e. the maximum of residual pore pressure (p_{\max}) increases with the increment of soil depth, is the same with that for the experimental measurements although there exist some differences between them for the maximum value of residual pore pressure.



(a) Time development of pore pressure at $z=-0.072\text{m}$ ($H=0.091\text{m}$).



(b) Vertical distributions of the maximum value of residual pore pressure.

Fig.3 Comparisons of pore pressure responses between the present numerical results and the experimental data from Sumer *et al.* (1999) ($T=1.6\text{s}$, $d=0.42\text{m}$, $L=2.89\text{m}$, $h=0.17\text{m}$, $G=5.4 \times 10^5 \text{ N/m}^2$, $k_s=5.37 \times 10^{-8}\text{m/s}$, $\mu=0.35$, $n=0.35$, $S_r=1.0$, $K_0=0.41$, $\alpha=0.48$, $\beta=0.29$).

Comparison of pore pressure responses in between the vicinity of pile foundation and the seabed without pile

In the current study, the pore pressure responses in the vicinity of pile foundations are investigated. Meanwhile, the corresponding results within seabed in the absence of pile are also obtained for comparison. The parameters for the numerical modeling are listed in Table 1.

Fig.4 shows the time developments of pore pressures at the center of the pile bottom (0, 0, -12m) and at the lateral surface of pile foundation (3, 0, -9m), where $D=6\text{m}$, $k_s=1.0 \times 10^{-4}\text{m/s}$. The corresponding results in the seabed without pile have been presented in the figure for comparison. It is seen from Fig.4 (a) that there are some differences for

the two cases. The residual component of pore pressure seems to be amplified due to the existence of pile foundation, whereas the amplitude of transient pore pressure is reduced. On the other hand, there are little differences for the variations of pore pressure with the time at the lateral position of pile foundation, compared with those in seabed without pile, as shown in Fig.4 (b). It is indicated that the existence of pile has some influences on the distribution of pore pressure in the vicinity of the bottom of the pile, but has little effects on those near the lateral position of the pile.

Table 1. Input data for present numerical study

<i>Wave characteristics</i>	
Wave period T	6.0 s
Water depth d	15.0 m
Wave length L	53.0 m
Wave height H	5.0 m
<i>Pile characteristics</i>	
Diameter D	6.0 m
Embedded depth l	(various in parametric study) 12.0 m
<i>Seabed properties</i>	
Seabed thickness h	24.0 m
Poisson's ratio μ	0.35
Soil porosity n	0.46
Shear modulus G	1.5×10^7 N/m ²
Permeability k_s	1.0×10^{-4} m/s (various in parametric study)
Unit weight of pore water γ_w	9.8×10^3 N/m ³
Submerged specific weight of soil γ'	10.73×10^3 N/m ³
Degree of saturation S_r	1.0
Coefficient of lateral earth pressure K_0	0.41
α	0.25
β	-0.29

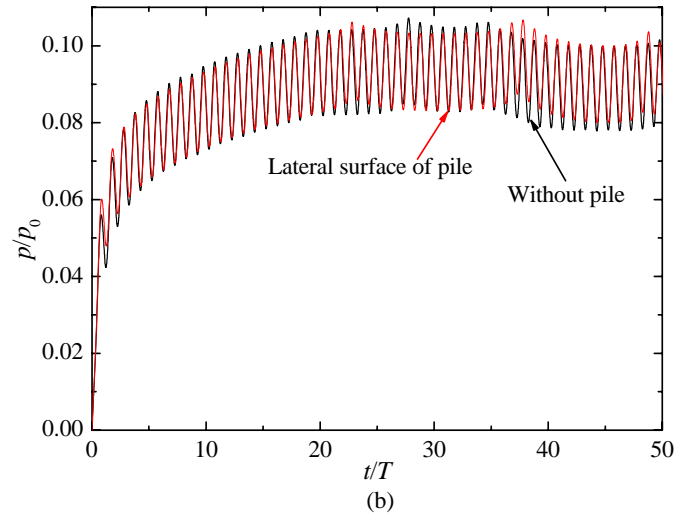
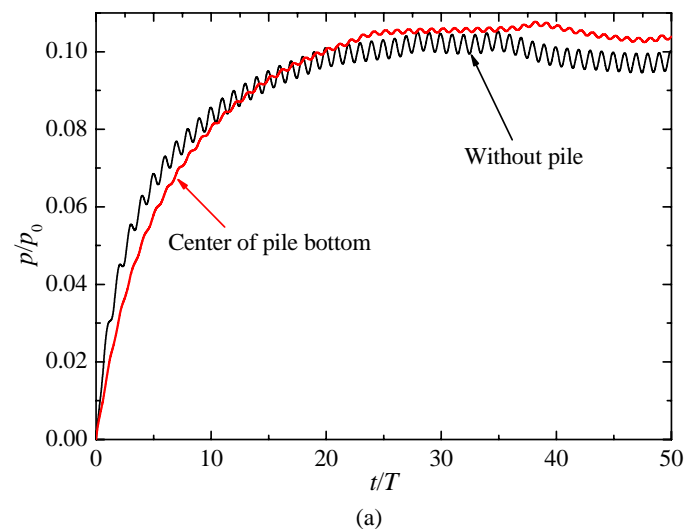
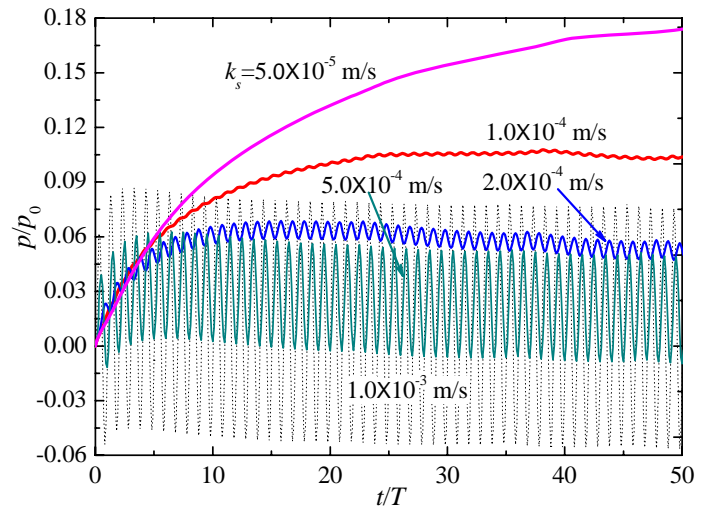


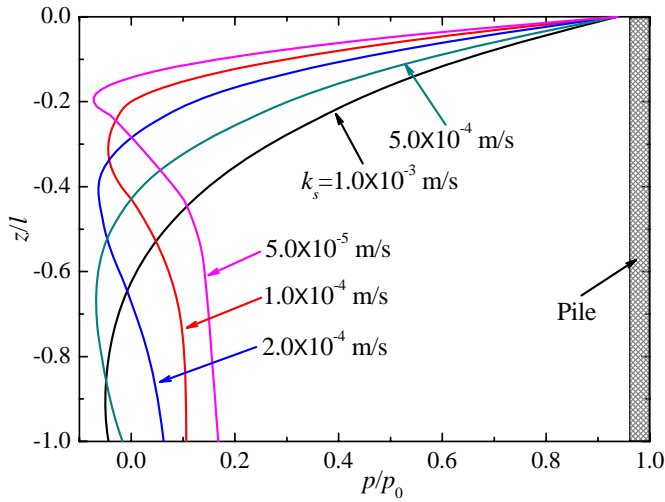
Fig. 4 Time developments of pore pressures in the vicinity of pile foundation and the seabed without pile: (a) Center of the bottom of pile at (0, 0, -12m); (b) Lateral surface of pile at (3, 0, -9m), where $D=6$ m, $k_s=1.0 \times 10^{-4}$ m/s.

Parametric study

Parametric study is carried out in this section to examine the influences of soil permeability k_s and pile diameter D on both transient and residual pore pressure responses around the pile foundation. The other parameters for the wave and the soil used in this study remained the same as shown in Table 1.



(a) Time developments of pore pressure at the center of the bottom of pile (0, 0, -12m), when $D=6$ m.

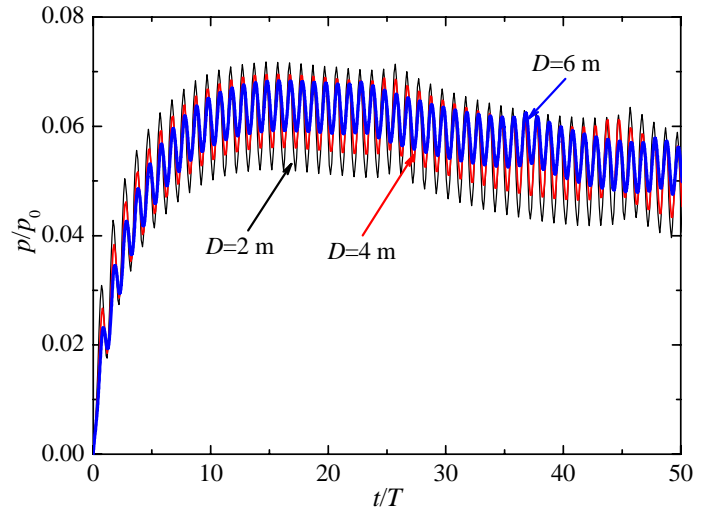


(b) Vertical distributions of pore pressure along the lateral surface of pile ($D=6\text{m}$).
 Fig. 5 Variations of pore pressure with change of soil permeability.

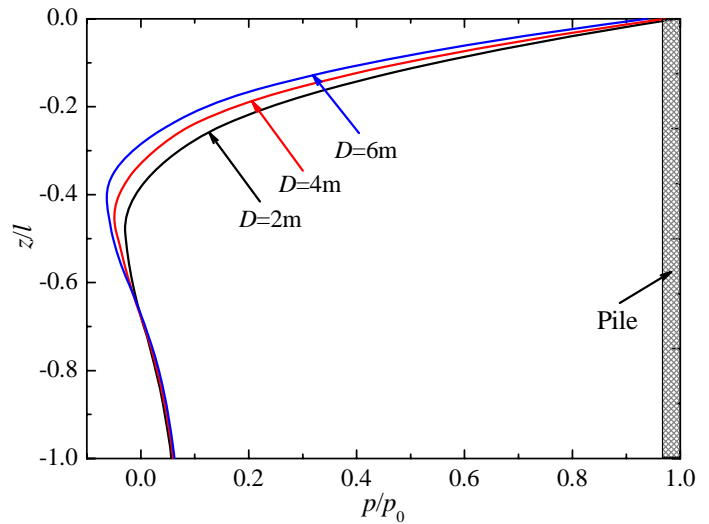
Fig. 5 presents the time developments of pore pressure at the center of the bottom of pile with diameter of 6m and the vertical distributions of pore pressure along the lateral surface of the pile foundation with different values of soil permeability k_s . As shown in Fig.5 (a), for $k_s = 1.0 \times 10^{-3}$ m/s, the residual pore pressure is not induced and the oscillatory component prevails. Whereas for $k_s = 5.0 \times 10^{-5}$ m/s, the build-up of residual pore pressure gets much more obvious. It is also indicated from the figure that pore pressure build-up increases gradually with the decrease of soil permeability. Moreover, the duration period for the pore pressure build-up to its maximum value decreases with the increase of soil permeability. Fig.5 (b) illustrates the vertical distributions of pore pressures along the lateral surface of the pile foundation with several values of soil permeability. All of them correspond to the time when pore pressure reaches the maximum at the position of the bottom of the pile. It can be seen that the attenuations of pore pressure are significant for all the cases in the upper half part of the pile, which may be due to the damping of amplitude and phase lag for the transient pore pressure within the seabed. Furthermore, the rate of the pore pressure attenuation is more obvious for smaller soil permeability. On the other hand, for the lower half part of the pile, in which transient component seems to decay to zero, residual pore pressure becomes dominated, and the pore pressure response increases with the decrease of soil permeability.

Fig. 6 shows the time developments of pore pressure at the center of the bottom of pile foundations and vertical distributions of pore pressure along the lateral surface of pile foundations with various pile diameters. As shown in Fig. 6(a), the diameter of pile foundation has an influence on the amplitude of transient pore pressure at the bottom of the pile, and the amplitude of transient pore pressure decreases with the increase of pile diameter. However, the value and rate of pore pressure build-up and dissipation are not very sensitive to the pile diameter. The reasons for that could be as follows: (i) the diameter of pile foundation is small relative to the wave length L (Here $D/L \approx 0.038, 0.075, 0.11$ respectively); (ii) the residual pore pressure has sufficient time to diffuse or spread within the seabed because of its larger time scale relative to the oscillatory pore pressure. Fig.6 (b) shows the vertical distributions of pore pressure along the lateral surface of the pile foundation at the moment when pore pressure arrives at the maximum at the bottom of the pile. It is indicated that at the upper half part of pile, the larger the pile diameter is, the faster the pore pressure attenuates; while at the lower half part of pile foundation, the pore pressure,

especially for the residual component, is not sensitive to the pile diameter.



(a) Time developments of pore pressure at the center of the bottom of pile foundations ($0, 0, -12\text{m}$), when $k_s = 2.0 \times 10^{-4}$ m/s.



(b) Vertical distributions of pore pressure along the lateral surface of pile, when $k_s = 2.0 \times 10^{-4}$ m/s.
 Fig. 6 Pore pressure variations with change of pile diameter

CONCLUDING REMARKS

A FEM model is presented to simultaneously simulate both residual and oscillatory pore pressure responses around pile foundations. The developed numerical model has been verified by the existing experimental data from Sumer *et al.* (1999).

The present numerical results indicate that the residual pore pressure response is significantly amplified at the bottom of pile foundation, whereas the amplitude of transient pore pressure at the same location decreases obviously, compared with those in the seabed without pile.

The soil permeability has significant influence on the residual and oscillatory pore pressure around the pile foundations. With the decrease of soil permeability, the build-up level of pore pressure increases, and

the rate of pore pressure development and the amplitude of transient pore pressure decrease. The effect of pile diameter on the oscillatory pore pressure is much more obvious than that on the build-up of residual pore pressure.

ACKNOWLEDGEMENTS

This work is financially supported by National Natural Science Foundation of China (Grant Nos. 10872198, 10902112), the Knowledge Innovation Program of Chinese Academy of Sciences (KJCX2-YW-L07) and the Scientific Research Foundation for the Returned Overseas Chinese Scholars, State Education Ministry.

REFERENCES

- Biot, MA (1941). "General theory of three-dimensional consolidation," *Journal of Applied Physics*, Vol 12, pp 155-164.
- DeAlba, P, Chan, CK, and Seed, HB (1975). "Determination of soil liquefaction characteristics by large scale laboratory tests," *Earthquake Engineering Research Center, University of California, Berkeley, Calif.*, Report No EERC 75-14.
- Jeng, DS, and Hsu, JRC (1996). "Wave-induced soil response in a nearly saturated seabed of finite thickness," *Geotechnique*, Vol 46, pp 427-440.
- Jeng, DS (1997). "Wave-induced seabed instability in front of a breakwater," *Ocean Engineering*, Vol 24, pp 887-917.
- Jeng, DS (2003). "Wave-induced seafloor dynamics," *Applied Mechanics Review*, Vol 56, No 4, pp 407-429.
- McDougal, WG, Tsai, YT, Liu, PL-F, and Clukey, EC (1989). "Wave-induced pore water pressure accumulation in marine soils," *Journal of Offshore Mechanics and Arctic Engineering*, Vol 111, pp 1-11.
- Nago, H, Maeno, S, Matsumoto, T, and Hachiman, Y (1993). "Liquefaction and densification of loosely deposited sand bed under water pressure variation," In: *Proceedings of the Third International Offshore and Polar Engineering Conference, Singapore*, pp 578-584.
- Rahman, MS, Seed, HB, and Brook, JR (1977). "Pore pressure development under offshore gravity structures," *Journal of the Geotechnical Engineering Division, ASCE*, Vol 103(GT 12), pp 1419-1437.
- Seed, HB, Martin, PQ, and Lysmer, J (1976). "Pore-water pressure changes during soil liquefaction," *Journal of the Geotechnical Engineering Division, ASCE*, Vol 102 (GT 4), pp 323-346.
- Seed, HB, and Rahman, MS (1978). "Wave-induced pore pressure in relation to ocean floor stability of cohesionless soils," *Marine Geotechnilogy*, Vol 3, No 2, pp 123-150.
- Sumer, BM, Fredsøe, J, Christensen, S, Lind, MT (1999). "Sinking-/floatation of pipelines and other objects in liquefied soil under waves," *Coastal Engineering*, Vol 38 No 2, pp 53-90.
- Sumer, BM, and Fredsøe, J (2002). "The mechanics of scour in the marine environment," *World Scientific, Singapore*, pp 464-482.
- Sumer, BM, Truelsen, C, and Fredsøe, J (2006). "Liquefaction around pipelines under waves," *Journal of Waterway Port Coastal and Ocean Engineering ASCE*, Vol 132, No 4, pp 266-75.
- Yamamoto, T, Koning, H, Sellneijer, H, and Van Hijum, E (1978). "On the response of a poroelastic bed to water waves," *Journal of Fluid Mechanics*, Vol 87, pp 193-206.
- Zienkiewicz, OC, and Scott, FC (1972). "On the principle of repeatability and its application in analysis of turbine and pump impellers," *International Journal for Numerical Methods in Engineering*, Vol 9, pp 445-452.